

Simultaneous sensing of temperature, CO, and CO₂ in a scramjet combustor using quantum cascade laser absorption spectroscopy

R. M. Spearrin · C. S. Goldenstein ·
I. A. Schultz · J. B. Jeffries · R. K. Hanson

Received: 14 March 2014 / Accepted: 17 June 2014 / Published online: 1 July 2014
© Springer-Verlag Berlin Heidelberg 2014

Abstract A mid-infrared laser absorption sensor was developed for gas temperature and carbon oxide (CO, CO₂) concentrations in high-enthalpy, hydrocarbon combustion flows. This diagnostic enables non-intrusive, in situ measurements in harsh environments produced by hypersonic propulsion ground test facilities. The sensing system utilizes tunable quantum cascade lasers capable of probing the fundamental mid-infrared absorption bands of CO and CO₂ in the 4–5 μm wavelength domain. A scanned-wavelength direct absorption technique was employed with two lasers, one dedicated to each species, free-space fiber-coupled using a bifurcated hollow-core fiber for remote light delivery on a single line of sight. Scanned-wavelength modulation spectroscopy with second-harmonic detection was utilized to extend the dynamic range of the CO measurement. The diagnostic was field-tested on a direct-connect scramjet combustor for ethylene–air combustion. Simultaneous, laser-based measurements of carbon monoxide and carbon dioxide provide a basis for evaluating combustion completion or efficiency with temporal and spatial resolution in practical hydrocarbon-fueled engines.

1 Introduction

Advancements in air-breathing supersonic propulsion systems have led to the need for a new generation of diagnostics to characterize the flow fields produced in these

devices. While extensive analytical research has been dedicated to hydrogen-fueled supersonic combustors, systems that utilize more practical hydrocarbon fuels have received growing interest of late [1]. Previous laser-based absorption diagnostics, typically probing water vapor, have proven valuable for assessing supersonic reacting gas systems [2–5]. Here, we extend absorption sensing in scramjets to the other major hydrocarbon combustion species, CO and CO₂. Previous measurements of CO₂ have been reported by Rieker et al. [6] in a vitiated scramjet, though limited to low temperatures by relatively weak near-infrared absorption above 600 K. This paper describes the development of a new mid-infrared quantum cascade laser absorption spectroscopy (QCLAS) sensor capable of providing non-intrusive, in situ measurements of temperature and carbon oxide species concentrations in high-speed hydrocarbon combustion flows. The sensor is initially targeted for scramjet combustor environments with further applicability to other high-temperature, short path-length (<5 cm) gas systems.

A scanned-wavelength direct absorption technique was primarily utilized, targeting rovibrational carbon monoxide (CO) and carbon dioxide (CO₂) transitions, near 4,854 and 4,176 nm, respectively. Temperature measurements were attained from the ratio of two CO transitions, and the thermometry range (~800–2,400 K) was enhanced in harsh environments by calibration-free second-harmonic detection using a wavelength modulation spectroscopy (WMS) technique. Two quantum cascade lasers are used in the sensor. The respective outputs of each laser were combined by free-space coupling to a bifurcated hollow-core fiber for remote light delivery. The fiber-coupled sensor was utilized to simultaneously measure temperature and species mole fractions in ethylene–air combustion conditions at multiple planes in the flow of a direct-connect

R. M. Spearrin (✉) · C. S. Goldenstein ·
I. A. Schultz · J. B. Jeffries · R. K. Hanson
High Temperature Gasdynamics Laboratory, Department
of Mechanical Engineering, Stanford University, Stanford,
CA 94305, USA
e-mail: spearrin@stanford.edu

model scramjet combustor at the University of Virginia. The diagnostic provides enhanced sensitivity to hydrocarbon combustion progress compared to analogous absorption sensing of water vapor.

2 Methods

2.1 Line selection

Recent availability of tunable, room-temperature quantum cascade lasers enable access to the strong mid-infrared absorption bands of CO and CO₂ centered near 4.6 and 4.3 μm, respectively [7]. These bands offer orders of magnitude greater absorption and more sensitive detection compared to the next strongest near-infrared bands for each species. Wavelength selection within each band is primarily influenced by the isolation, strength, and temperature sensitivity of the discrete rovibrational lines that compose the bands, as well as laser availability. Figure 1 shows the fundamental absorption bands for CO and CO₂ plotted as line-strengths at 2,000 K [8]. At combustion temperatures, we note the P-branch of CO₂ and the R-branch of CO interfere spectrally, and this overlapping domain was avoided for line selection. Two neighboring lines are chosen from the more isolated P-branch of the fundamental carbon monoxide band near 2,059.9 and 2,060.3 cm⁻¹ to infer temperature and CO mole fraction. The proximity of these wavelengths (~0.4 cm⁻¹) allows for a two-line measurement with a single laser. Though not shown in the figure, water vapor interference further constrained line selection for CO, and the chosen line-pair exhibits excellent isolation relative to other candidate transitions [9]. Carbon dioxide mole fraction is measured by probing a temperature-insensitive R-branch transition in the fundamental band near 2,394.4 cm⁻¹. The selected CO₂ line is near the fundamental bandhead, which involves tight line spacing as evidenced by the dense (solid red) spectra in Fig. 1, and benefits from excellent spectral isolation from water vapor and CO₂ hot bands [10]. Relevant spectroscopic data are presented in Table 1 for the three selected transitions. Line -strength and lower-state energy values for CO and CO₂ transitions, especially in the fundamental bands, are generally well known due to the simple structure of the molecules [11, 12], and taken here from the HITEMP 2010 database [8].

2.2 Laser absorption spectroscopy

Scanned-wavelength absorption spectroscopy techniques were used in this work to determine thermodynamic properties of interest from the measured absorption spectra. A brief discussion of the theoretical framework is provided

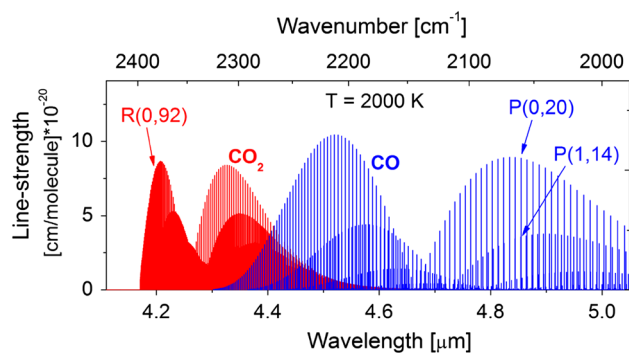


Fig. 1 Absorption line-strengths for CO and CO₂ from 4 to 5 μm; $T = 2,000$ K; transitions labeled as branch (ν'' , J'')

here to define units and nomenclature. The Beer–Lambert law, given by Eq. 1, provides the fundamental relation governing narrow-band light absorption across a uniform gas medium

$$\alpha_\nu = -\ln\left(\frac{I_t}{I_0}\right)_\nu = S_j(T)\varphi_\nu(T, P, \chi)Px_{\text{abs}}L. \quad (1)$$

Measured quantities of incident and transmitted light intensities define the spectral absorbance, α_ν , at frequency ν , which is further related to the product of spectroscopic line parameters (S_j , φ_ν), the partial pressure of the absorbing species, and the optical path-length. By scanning the lasers in wavelength across each discrete transition j , the often complex dependence on the spectral line-shape, φ_ν , can be eliminated, simplifying the measurement to an integrated absorbance area, A_j , which is only reliant on a single spectroscopic parameter, the line-strength, $S_j(T)$, as expressed in Eq. 2.

$$A_j = \int_{-\infty}^{\infty} \alpha_\nu d\nu = S_j(T)Px_{\text{abs}}L. \quad (2)$$

The ratio of integrated absorbance of two transitions further simplifies to a ratio of line-strengths R , which is a function of temperature only. With the lower-state energy and line-strength at a reference temperature known for each transition (see Table 1), the simultaneous measure of two lines of a single species facilitates direct inference of gas temperature. The temperature sensitivity of the line-strength ratio $(dR/R)/(dT/T)$, for a given pair of lines (A and B) can be expressed as

$$\left|\frac{dR/R}{dT/T}\right| = \left(\frac{hc}{k}\right) \frac{|E''_A - E''_B|}{T} \quad (3)$$

where h (J s) is Planck's constant, c (cm/s) is the speed of light, k (J/K) is Boltzmann's constant, and E'' (cm⁻¹) is the lower-state energy for the target absorption lines [13]. As defined in Eq. 3, the difference in lower-state energies between the two selected transitions governs the

Table 1 Spectroscopic parameters of CO and CO₂ transitions used in the present sensor

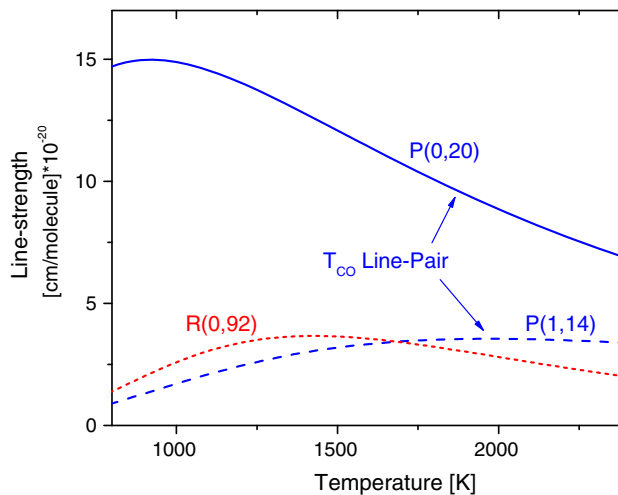
Line assignment branch (v'' , J'')	Species	Wavelength (nm)	Frequency (cm ⁻¹)	E'' (cm ⁻¹)	S (296 K) (cm ⁻² /atm)
$P(0, 20)$	CO	4,855	2,059.91	806.4	87.6×10^{-2}
$P(1, 14)$	CO	4,854	2,060.33	2,543.1	26.4×10^{-5}
$R(0, 92)$	CO ₂	4,176	2,394.42	3,329.0	73.9×10^{-6}

temperature sensitivity for two-line thermometry. The selected CO line-pair has a lower-state energy difference of $\Delta E'' = 1,737 \text{ cm}^{-1}$, which yields a temperature sensitivity of greater than unity up to 2,500 K. With temperature measured, species mole fraction can be obtained from the absorption of either transition with concurrent knowledge of pressure and path-length per Eq. 2. Integrated absorbance areas for each line were determined by Voigt line-shape fitting methods. The primary technique, scanned-wavelength direct absorption (DA), involved directly fitting the Voigt function to measured absorbance profiles, which is a relatively simple and well-established method [14]. In addition, a recently developed scanned-WMS technique was employed to extract the absorbance area by fitting a $1f$ -normalized second-harmonic ($2f$) profile, extending the dynamic range of the CO temperature measurement by enhanced noise suppression. Details on this technique are found in a separate publication by Goldenstein et al. [15]. These laser techniques and spectroscopic parameters were validated in a heated static optical cell over a range of temperatures (500–800 K) and pressures (0.5–2 bar) prior to field deployment of the sensor, with typical measurement uncertainty of $\pm 2 \%$ for each species.

2.3 Optimization for non-uniform flows

In the scramjet combustor, as in most propulsion applications, the path-length or line of sight (LOS) over which the measurement is performed may involve gradients in gas properties. Though sometimes, these gradients can be negligible, in many cases, flow non-uniformities can convolute LOS measurement schemes and distort quantitative results. Here, we briefly describe the strategic approach for these LOS measurements in the scramjet environment that minimizes sensitivity to non-uniformities. A previous paper [16] has been dedicated to this topic, so here we constrain the discussion to our particular application.

The species-specific nature of laser absorption spectroscopy lends to species-weighted measurements, implying that measurements of gas properties such as temperature will be weighted toward regions of the flow wherein the species being probed has a higher density and absorption strength. Previous research has been aimed at quantifying non-uniformities for LOS measurements [17–19]. The goal here was to obtain a species-weighted path-average measurement that serves as a

**Fig. 2** Line-strengths versus temperature for the selected CO (blue) and CO₂ (red) transitions

metric that can be readily compared to computational modeling. To obtain a path-average measurement, our strategy is to probe a spectroscopic quantity that has a linear dependence on the non-uniform gas properties, namely temperature, pressure, and mole fraction. As defined in Eq. 2, the integrated absorbance area provides an ideal parameter for non-uniform gases due to the simple linear relationship with pressure, mole fraction, path-length, and line-strength. The scanned-wavelength techniques described in the previous section (DA and WMS) are thus both designed to yield the integrated absorbance area via a Voigt fitting routine. Further, to obtain a linear dependence on temperature, transitions should be selected to have a line-strength which is linear with temperature over the target temperature range as discussed by Goldenstein et al. [16]. Figure 2 shows the three lines selected for this sensor plotted as a function of temperature (800–2,400 K). The $P(0, 20)$ and $P(1, 14)$ lines of CO exhibit a nearly linear and inverse relationship over the temperature range of 1,500–2,000 K, the primary range of interest. The $R(0, 92)$ line of the CO₂ fundamental band was chosen due to insensitivity to temperature over a broad range of high temperature. Line-strength for the CO₂ transition varies less than $\pm 10 \%$ from 1,200 to 1,850 K. Such insensitivity is advantageous for the CO₂ concentration measurement to negate the effect of temperature non-uniformity and also because the temperature being used to infer concentration here is that measured from CO, which may be

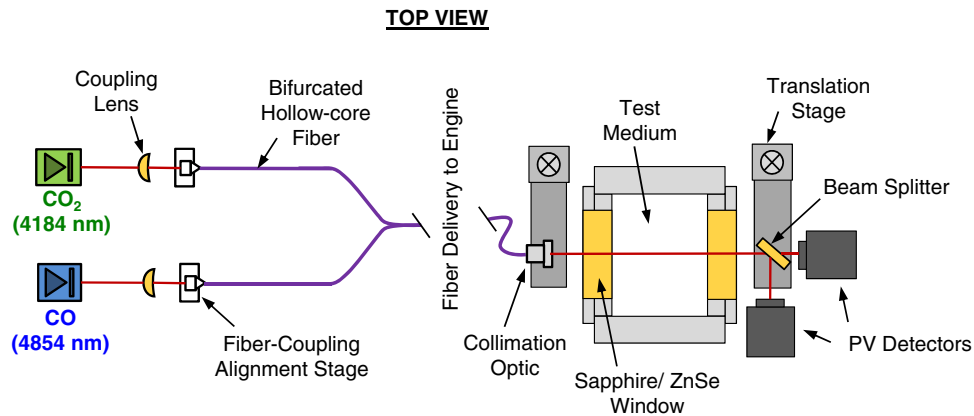


Fig. 3 Optical configuration for free-space fiber-coupling (*left*) and cross section of scramjet combustor showing remote light delivery and collection (*right*). Flow direction is out of the page

slightly different than the CO₂ temperature due to variable distributions of the molecules along the line of sight. Such careful consideration of the laser technique and line selection enhances the quantitative value of these LOS absorption measurements.

3 Experimental setup

3.1 Optical hardware

Figure 3 provides a graphical depiction of the optical configuration for the multi-species laser absorption sensor. For carbon monoxide, a distributed-feedback (DFB) quantum cascade laser (ALPES) near 4,860 nm provides a single-mode light source with ~ 10 mW output power. An external-cavity quantum cascade laser (Daylight Solutions) centered near 4,250 nm provides single-mode light at 30 mW nominal output power for probing the carbon dioxide spectra. Each incident beam is free-space coupled into a 1.25 m bifurcated hollow-core fiber (OKSI, $d = 300$ μm), which combines the beams into a parallel and near co-linear path (300 μm core diameter separation) for pitching across the test medium. Net transmission through the fiber is better than 50 % for each wavelength. The fiber output is then re-collimated using a plano-convex silicon lens ($f.l. = 40$ mm) and transmitted through a wedged sapphire window. The combined beam, after passing through the test medium, is de-multiplexed using an anti-reflection coated CaF₂ beam splitter, and spectrally bandpass filtered (~ 50 nm) for each respective wavelength, followed by collection on two infrared thermoelectrically cooled photovoltaic detectors (Vigo PVI-4TE-5). The detectors have a bandwidth of 10 MHz and 2 mm² detection area ($D^* \geq 3 \times 10^{11}$ cm Hz^{1/2} W⁻¹).

For direct absorption measurements, the CO DFB laser is centered at 2,060.2 cm⁻¹ and scanned at 6 kHz (sawtooth)

with an injection current amplitude of 80 mA, yielding a scan range of approximately 0.9 cm⁻¹ to capture both the $P(0, 20)$ and $P(1, 14)$ carbon monoxide transitions in a single laser scan. The external-cavity CO₂ QCL is centered at 2,394.4 cm⁻¹ and piezo-electrically scanned at 100 Hz (sine wave), yielding a scan range of approximately 1 cm⁻¹. Prior to and between tests, the respective beams are redirected to a wavemeter (Bristol 621B) to confirm center wavelength. A germanium Fabry–Pérot etalon, with a free-spectral range (FSR) of 0.016 cm⁻¹, enabled data conversion from the time to wavelength domain.

In WMS measurements, the DFB-QCL for carbon monoxide was modulated rapidly at 50 kHz and simultaneously scanned more slowly (sine wave) at 200 Hz to capture the two P-branch lines. A modulation depth of 0.057 cm⁻¹ was chosen to maximize the peak second-harmonic signal for the conditions expected in the scramjet. The lock-in amplifier outputs, namely the first and second-harmonic signals, were low-pass filtered at 10 kHz. To eliminate dependence on the absolute optical power, the $2f$ signal is normalized by the $1f$ signal. This normalization mitigates baseline uncertainties resulting from scattering, window fouling, and beam steering [9].

3.2 Facility interface

Initial field measurements using this sensor were carried out at the University of Virginia Supersonic Combustion Facility (UVaSCF) [20]. The direct-connect combustor was oriented vertically, with continuous air flow provided by a compressor and underground heater system. Air out of the heater had a total temperature of 1,200 K and was expanded by a nozzle to Mach 2 conditions prior to entering the combustor. Heated ethylene was injected through five ports located approximately 2.5 cm upstream of a cavity flame holder [21, 22]. The optical LOS was transverse to the injector with a path-length of 3.81 cm corresponding to the cross-sectional width

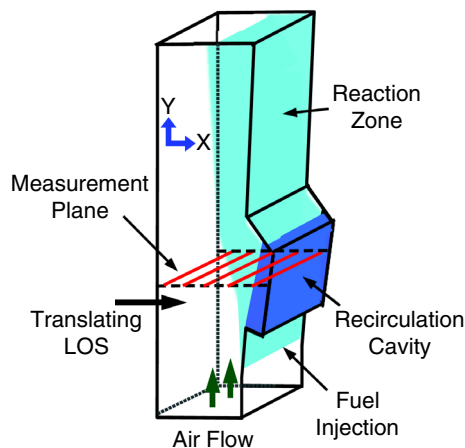


Fig. 4 UVaSCF supersonic combustor schematic; example optical lines of sight shown in red

of the combustor. Position of the optical LOS in the x - y plane was controlled by a set of high-precision translation stages (Zaber). Figure 4 illustrates a basic schematic of the combustor with representative optical lines of sight across a transverse measurement plane. Demonstration data shown in the subsequent section was taken in the combustor cavity plane approximately 2.18 cm downstream of the cavity leading edge.

During combustor operation, a number of harsh thermo-mechanical phenomena were introduced to the ambient environment that required mitigation for successful sensor employment. To counter mechanical vibrations and acoustic perturbations, the lasers were mounted to a honeycomb vibration-dampening breadboard. Due to radiation emitted by the combustor, the photovoltaic detectors were mounted to water-cooled plates to prevent saturation or damage from overheating. Heating in the room also led to elevated levels of water vapor in the humid ambient air, which could spectrally interfere with the absorption measurements and condense on cooled optical equipment. A nitrogen purge of the optical breadboard was constructed to minimize this water vapor. The N₂ purge was extended to the hollow-core fiber and optical detection components as well to encompass the entire optical path of each laser output.

4 Results

The present mid-infrared sensor aimed to measure gas temperature, carbon monoxide, and carbon dioxide simultaneously with both temporal and spatial resolution in the harsh combustion environment. Raw data quality for direct absorption measurements can be examined by inspection of the laser scans, exhibited in Figs. 5a and 6a, for CO and CO₂, respectively. Transmitted laser light intensity, in detected volts, is shown along with the baseline intensity,

which was captured after flame extinction. For the DFB-QCL dedicated to CO measurements, the sawtooth scan (see Fig. 5a) was deliberately set to go below the threshold current of the laser for a short time, during which thermal emission could be measured and subtracted from the adjacent signal. For the ECQCL dedicated to CO₂, the piezo-scan simply tunes a mechanical grating such that laser output intensity is nearly constant across the laser scan (see Fig. 6a). Therefore, to account for thermal emission, a beam chopper (~ 12.5 Hz) was mounted at the output of the ECQCL to intermittently block the laser after every eight scans for a period of ~ 5 ms wherein thermal emission was measured and subtracted in a similar manner as described above. Due to the temperature- and wavelength-dependent transmission of the sapphire windows, the baseline, which was measured at a lower temperature after combustion ceased, was scaled to match the non-absorbing regions of the transmitted intensity scan. Both thermal emission and window losses were noted to change on sufficiently slow time scales that these effects were effectively constant during a single laser scan. Figures 5b and 6b show the conversion of the raw intensity signals to absorbance and transposed to the wavenumber domain, from which the Voigt line-shape function could be fit to each transition to yield the integrated absorbance areas.

Since line-strengths are well known for the selected transitions, the quality of the baseline and Voigt fits typically limit measurement uncertainty for scanned-wavelength direct absorption techniques in harsh, turbulent environments. Non-gaussian noise sources in the baseline may be manifested by systematic drift of detected signal during the laser scan period, such as beam steering or other fluctuations at a similar frequency as the laser scan frequency. With such large absorbance in this application, these uncertainties were relatively small in most measurement locations and can be partly quantified by inspection of the residual to the Voigt fit, displayed in Figs. 5 and 6 as percent of peak absorbance. For CO detection, both lines as depicted in Fig. 5b exhibit SNR >30 with minimal systematic baseline error (i.e., <1 % baseline drift and <1 % residual noise in non-absorbing regions). The baseline shifting and scaling process was highly repeatable scan to scan and <3 % overall measurement uncertainty was introduced for the determination of integrated areas at nominal concentrations in the combustor cavity. For the two-line CO temperature measurement, this translates to <3 % temperature uncertainty below 2,500 K at a nominal mole fraction ($X_{\text{CO}} \sim 0.05$). The SNR was observed to degrade nearly linearly with mole fraction, yielding a CO detection limit of $\sim 1,000$ ppm at 6 kHz using the stronger $P(0, 20)$ line. The carbon dioxide measurements were more prone to baseline distortion resulting from random fluctuations in laser

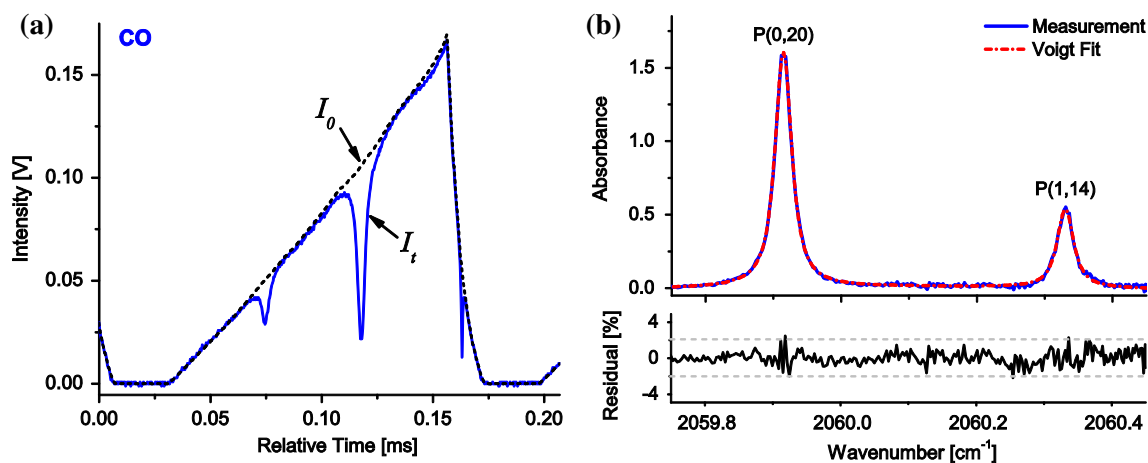


Fig. 5 Measured carbon monoxide absorption from a single laser scan (6 kHz) shown as **a** raw voltage signals versus time and **b** absorbance versus wavenumber; $T = 1,725$ K, $P = 0.71$ bar, $L = 3.81$ cm, $X_{\text{CO}} = 0.057$; $\varphi \approx 0.15$, measurement taken 2.18 cm downstream of cavity leading edge, 1 mm from cavity wall

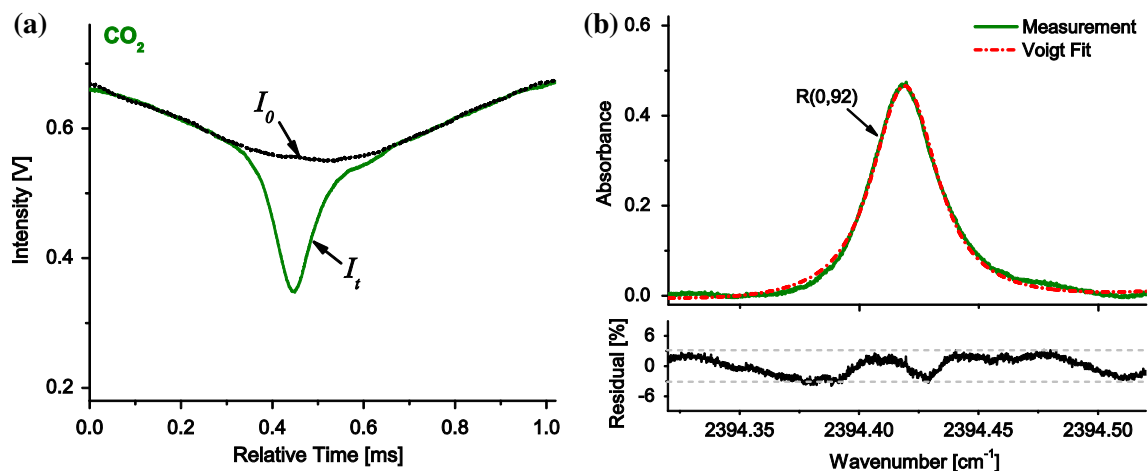


Fig. 6 Measured carbon dioxide absorption from a single laser scan (100 Hz) shown as **a** raw voltage signals versus time and **b** absorbance versus wavenumber; $T = 1,725$ K, $P = 0.71$ bar, $L = 3.81$ cm, $X_{\text{CO}_2} = 0.062$; $\varphi \approx 0.15$, measurement taken 2.18 cm downstream of cavity leading edge, 1 mm from cavity wall (same as Fig. 5)

output power ($\sim 2\%$) due to sensitivity of the ECQCL to mechanical vibrations. This noise source, notable in the residual plot in Fig. 6b, appeared larger in amplitude compared to beam steering, which was independently observed in the shared LOS with the CO beam, and also dominates interference absorption ($<1\%$) from neighboring CO_2 lines. Although such vibration-induced intensity fluctuations were random, the baseline fitting uncertainty limited overall CO_2 measurement uncertainty to 5%. Based on noise alone, a detection limit of $\sim 1,200$ ppm CO_2 was achieved (SNR ~ 1).

The scanned-WMS technique, implemented with the DFB-QCL for CO, further suppressed measurement noise. Figure 7a shows an example scan of the raw WMS data for CO, taken at a similar operating condition and spatial

location as the data presented in Fig. 5. The absorption from each of the two P-branch lines can be observed, centered in the sinusoidal half-scan (200 Hz). With the modulation depth predetermined in the laboratory, the normalized second harmonic can be plotted against wavenumber as shown in Fig. 7b. As previously mentioned, the Voigt fitting routine to the background WMS signal renders the integrated absorbance areas when matched to the measured data. The fitted $2f$ line-shape for each transition can be seen in the figure compared to the measured line-shapes. This WMS technique was implemented to enhance the dynamic range of the temperature measurement, which is limited by the weaker $P(1, 14)$ line. Although CO mole fraction can be calculated with an estimated temperature and the $P(0, 20)$ line alone, temperature requires the line-

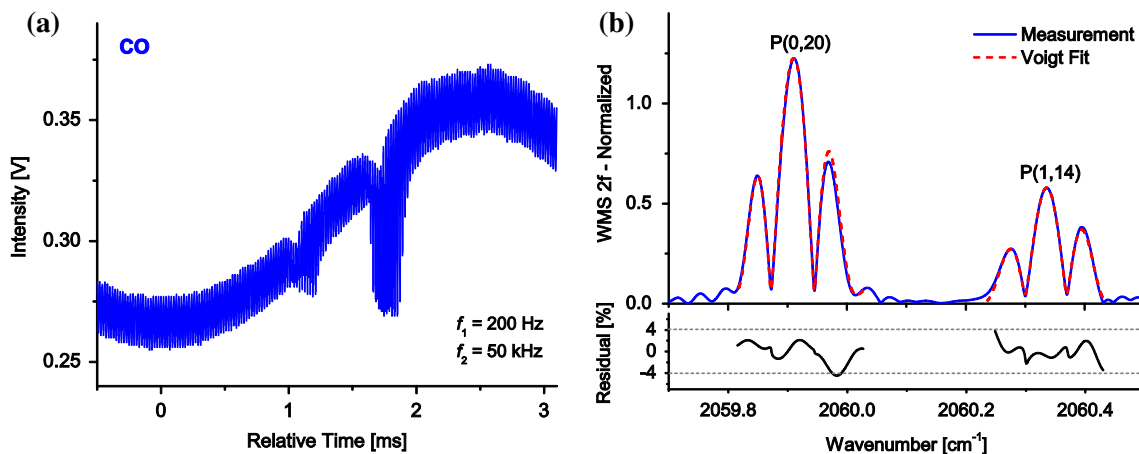


Fig. 7 Measured carbon monoxide wavelength modulation scan (50 kHz, 200 Hz) shown as **a** raw voltage signal versus time and **b** normalized second-harmonic signal versus wavenumber; $T = 1,690$ K, $P = 0.71$ bar, $L = 3.81$ cm, $X_{CO} = 0.063$; $\varphi \approx 0.15$, measurement taken 2.18 cm downstream of cavity leading edge, 1 mm from cavity wall

pair. Utilizing the WMS line-shape fitting method, temperature could be determined at CO concentrations approximately 3 times lower ($\sim 1,000$ ppm limit for T_{CO} , ~ 350 ppm for X_{CO}) than with direct absorption, determined by the noise floor at 200 Hz of the normalized $2f$ signal (SNR ~ 1).

4.1 Time-resolved measurements

The time resolution of each species measurement is equivalent to the scan rate of each QCL that comprises the sensor: 6 kHz or 200 Hz for CO, and 100 Hz for CO₂. Such bandwidths, especially for the faster CO DFB laser, can provide valuable time-resolved information about flow field properties. Figure 8 shows the integrated absorbance areas for each of the two CO transitions, measured at a fixed x - y location in the combustor cavity during ethylene-air combustion conditions ($\varphi = 0.15$). Each data point represents the result from a single laser scan as described above. The integrated areas are observed to vary dramatically ($>25\%$) during the acquired test time (1 s). The positively correlated trends over time between the $P(0, 20)$ and $P(1, 14)$ areas supports the physical natural of this fluctuation. We further note that the physical oscillations in temperature at a fixed position in the combustor are much smaller ($<10\%$) than the fluctuations in mole fraction, which scales linearly with absorbance area and is shown on a longer time scale, along with CO₂ mole fraction, in Fig. 9. Further, it is noted that the variation in CO appears much larger than the variation in CO₂ at the respective bandwidths of each sensor, but when applying a moving average to the CO mole fraction data to yield a 100 Hz bandwidth, the fluctuations become very similar ($\sim 15\%$). For both temperature and species concentrations, these

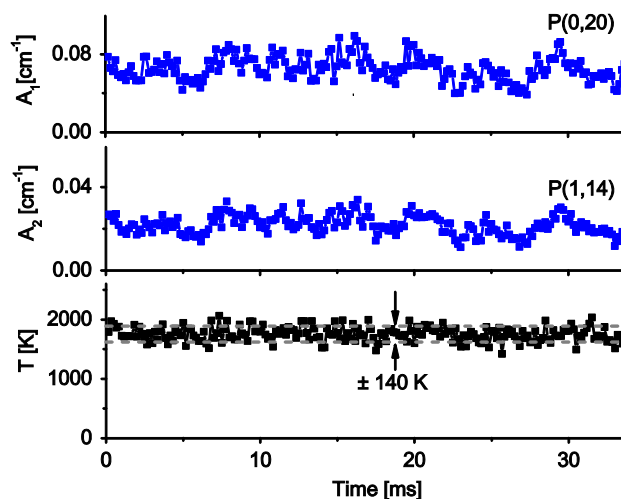


Fig. 8 Representative time-resolved CO absorbance areas and temperature at a fixed x - y position in the combustor cavity; ethylene-air, $\varphi = 0.15$; measurement taken 2.18 cm downstream of cavity leading edge, 1 mm from cavity wall

physical variations are greater than measurement uncertainties described in the previous section. Similar fluctuations in both temperature and mole fraction were noted in independently conducted water vapor absorption measurements [23]. The time-resolved carbon oxide data provide a basis to evaluate combustion stability and gas dynamic events.

4.2 Spatially resolved measurements

In addition to high-bandwidth measurements, the current experimental setup facilitates carbon oxide sensing with 2D spatial resolution. The translation stages can position the optical line of sight along a plane transverse to the bulk

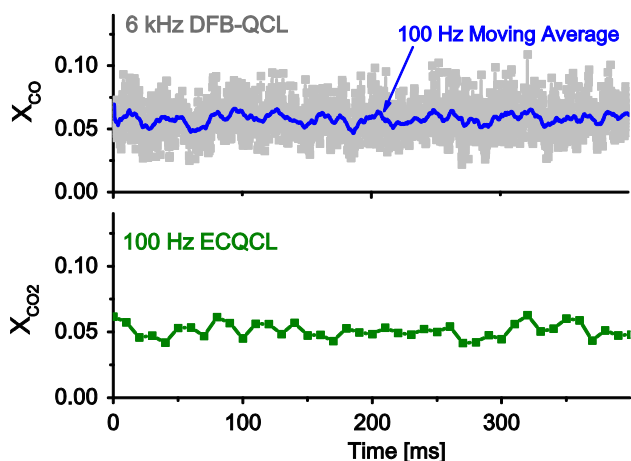


Fig. 9 Representative time-resolved CO and CO₂ mole fraction data at a fixed x - y position in the combustor cavity; ethylene–air, $\phi = 0.15$; measurement taken 2.18 cm downstream of cavity leading edge, 1 mm from cavity wall

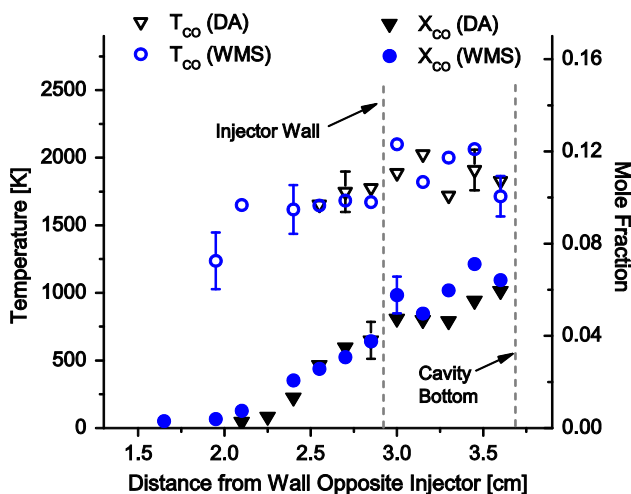


Fig. 10 Comparison of DA and WMS measurements of temperature and CO mole fraction across the cavity plane at $\phi = 0.15$

flow (x -axis) as illustrated in Fig. 4 and at multiple planes along the flow direction (y -axis). Figure 10 provides an example of the spatially resolved CO data across a transverse plane in the model scramjet combustor at an axial location in the flame-holding cavity (see Fig. 4). All data points are time-averaged over approximately one second, and the error bars represent the standard deviation (physical oscillations) over this time interval. The data illustrate the relative range and agreement between the DA and WMS techniques for measurements of temperature and CO mole fraction at the same operating condition ($\phi = 0.15$). Overall, the two techniques were observed to generally agree within the time-variable uncertainty of the measurements due to the unsteady nature of the flame,

especially considering that the measurements were taken several minutes apart. It can be noted, however, that the agreement outside of the turbulent flame-holding cavity tends to be better for both temperature and species mole fraction. Moreover, we can observe that the WMS technique enhances the measurement range, especially for temperature, further into the free stream where less CO is present.

Of particular importance, spatially resolved species measurements in the combustor facilitate assessment of flame structure and combustion progress. Figure 11 shows data of CO and CO₂ mole fraction measured across the transverse cavity plane. The two plots represent a snapshot of the same measurement plane under different fuel to air mass flow ratios ($\phi_a = 0.15$ and $\phi_b = 0.21$). All data points are similarly time-averaged as previously mentioned. Water concentration, which was measured independently at the same test conditions [23], is also shown for reference.

Though combustor analysis is reserved for another publication in the aerospace literature [24], these example data highlight the value of this in situ carbon oxide sensor, and a few observations deserve mention. We observe that conditions in the cavity appear near stoichiometric or rich, while carbon oxides become quickly diluted once entering the free stream, both trends that would be expected. Comparing the aggregate carbon oxide concentration with values of independently measured H₂O, we find excellent consistency with C₂H₄ atom balance ($X_{CO} + X_{CO_2} = X_{H_2O}$) for both conditions, even while relative carbon oxide levels vary considerably between equivalence ratios. These observations provide physical validation to the measurements, but also point to the strength and sensitivity of the diagnostic approach. At $\phi = 0.15$, peak CO and CO₂ mole fractions are both near 6%, while at $\phi = 0.21$, the peak values are approximately 10 and 3%, respectively. Similarly, comparing the H₂O measurements across equivalence ratios, we note that mole fractions peak around 12% (a near stoichiometric level) for both conditions, suggesting that the CO and CO₂ measurements are each a more sensitive measure of combustion progress for ethylene–air. Moreover, due to the inverse relationship of CO and CO₂ with combustion progress, the combined measurement (CO:CO₂ ratio) yields even greater sensitivity. These observations reinforce the strength of the two-species carbon oxide sensing strategy for assessing hydrocarbon combustion.

5 Summary

A mid-infrared quantum cascade laser absorption sensor was developed for simultaneous measurements of carbon monoxide, carbon dioxide, and gas temperature in supersonic propulsion flows. Two QCLs comprised the sensor, coupled

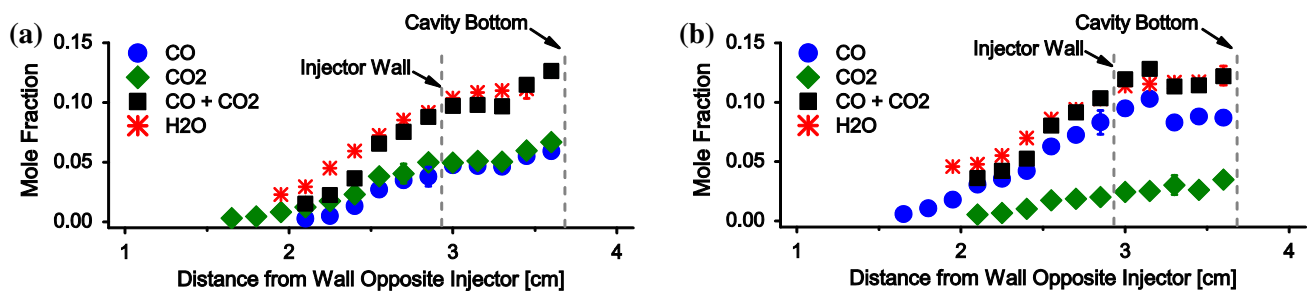


Fig. 11 Carbon oxide mole fraction measurements across the cavity plane for ethylene–air combustion at **a** $\phi = 0.15$ and **b** $\phi = 0.21$. $X_{\text{H}_2\text{O}}$ also shown

with a bifurcated hollow-core fiber for remote light delivery. The sensor was successfully demonstrated at the University of Virginia's direct-connect scramjet combustor facility for time-resolved detection (up to 6 kHz) at multiple fuel–air flow ratios, with detection limits of $\sim 1,000$ ppm for each species at the ~ 4 cm path-length. Utilization of WMS enhanced noise rejection compared to direct absorption and extended the useful range of the temperature measurement. Spatially resolved species measurements across the combustor highlighted the sensitivity of a combined CO/CO₂ sensor to hydrocarbon combustion progress. To the authors' knowledge, these measurements represent the first combined, in situ detection of CO and CO₂ in a scramjet combustor. Furthermore, the proven utilization of novel mid-infrared light sources and fiber optics in a harsh environment provides a sensor design framework by which similar mid-infrared diagnostics may be developed for future studies.

Acknowledgments This work was sponsored by the National Center for Hypersonic Combined Cycle Propulsion (NCHCCP), Grant FA 9550-09-1-0611, with technical monitors Chiping Li (AFOSR) and Rick Gaffney (NASA). The authors would also like to thank Bob Rockwell, Brian Rice, and Roger Reynolds of the University of Virginia for their assistance in operating the UVaSCF facility.

References

- J.M. Tishkoff, J.P. Drummond, T. Edwards, A.S. Nejad, in *Future Directions of Supersonic Combustion Research—Air Force/NASA Workshop on Supersonic Combustion*. 35th Aerospace Sciences Meeting and Exhibit (1997)
- G. Rieker, J. Jeffries, R. Hanson, T. Mathur, M. Gruber, C. Carter, Diode laser-based detection of combustor instabilities with application to a scramjet engine. *Proc. Combust. Inst.* **32**, 831–838 (2009)
- J.T.C. Liu, G.B. Rieker, J.B. Jeffries, M.R. Gruber, C.D. Carter, T. Mathur, R.K. Hanson, Near-infrared diode laser absorption diagnostic for temperature and water vapor in a scramjet combustor. *Appl. Opt.* **44**, 6701 (2005)
- F. Li, X. Yu, H. Gu, Z. Li, Y. Zhao, L. Ma, L. Chen, X. Chang, Simultaneous measurements of multiple flow parameters for scramjet characterization using tunable diode-laser sensors. *Appl. Opt.* **50**, 6697–6707 (2011)
- A. Griffiths, A. Houwing, Diode laser absorption spectroscopy of water vapor in a scramjet combustor. *Appl. Opt.* **44**, 6653–6659 (2005)
- G.B. Rieker, J.B. Jeffries, R.K. Hanson, Calibration-free wavelength-modulation spectroscopy for measurements of gas temperature and concentration in harsh environments. *Appl. Opt.* **48**, 5546 (2009)
- K. Namjou, S. Cai, E.A. Whittaker, J. Faist, C. Gmachl, F. Capasso, D.L. Sivco, A.Y. Cho, Sensitive absorption spectroscopy with a room-temperature distributed-feedback quantum-cascade laser. *Opt. Lett.* **23**, 219 (1998)
- L.S. Rothman, I.E. Gordon, R.J. Barber, H. Dothe, R.R. Gamache, A. Goldman, V.I. Perevalov, S.A. Tashkun, J. Tennyson, HITEMP, the high-temperature molecular spectroscopic database. *J. Quant. Spectrosc. Radiat. Transf.* **111**, 2139–2150 (2010)
- R.M. Spearrin, C.S. Goldenstein, J.B. Jeffries, R.K. Hanson, Quantum cascade laser absorption sensor for carbon monoxide in high-pressure gases using wavelength modulation spectroscopy. *Appl. Opt.* **53**, 1938–1946 (2014)
- R.M. Spearrin, W. Ren, J.B. Jeffries, R.K. Hanson, Multi-band infrared CO₂ absorption sensor for sensitive temperature and species measurements in high-temperature gases. *Appl. Phys. B* (2014). doi:10.1007/s00340-014-5772-7
- L. Rosenmann, S. Langlois, C. Delaye, J. Taine, Diode laser measurements of CO₂ line intensities at high temperature in the 4.3 μm region. *J. Mol. Spectrosc.* **149**, 167–184 (1991)
- P.L. Varghese, R.K. Hanson, Tunable infrared diode laser measurements of line strengths and collision widths of 12C16O at room temperature. *J. Quant. Spectrosc. Radiat. Transf.* **24**, 479–489 (1980)
- X. Zhou, X. Liu, J.B. Jeffries, R.K. Hanson, Development of a sensor for temperature and water concentration in combustion gases using a single tunable diode laser. *Meas. Sci. Technol.* **14**, 1459–1468 (2003)
- U. Platt, J. Stutz, *Differential Optical Absorption Spectroscopy: Principles and Applications* (Springer, Berlin, 2008), p. 597
- C.S. Goldenstein, C.L. Strand, I.A. Schultz, K. Sun, J.B. Jeffries, R.K. Hanson, Fitting of calibration-free scanned-wavelength-modulation spectroscopy spectra for determination of gas properties and absorption lineshapes. *Appl. Opt.* **53**, 356–367 (2014)
- C.S. Goldenstein, I.A. Schultz, J.B. Jeffries, R.K. Hanson, Two-color absorption spectroscopy strategy for measuring the column density and path average temperature of the absorbing species in nonuniform gases. *Appl. Opt.* **52**, 7950–7962 (2013)
- X. Ouyang, P.L. Varghese, Line-of-sight absorption measurements of high temperature gases with thermal and concentration boundary layers. *Appl. Opt.* **28**, 3979–3984 (1989)
- S.T. Sanders, J. Wang, J.B. Jeffries, R.K. Hanson, Diode-laser absorption sensor for line-of-sight gas temperature distributions. *Appl. Opt.* **40**, 4404 (2001)
- L. Ma, X. Li, S.T. Sanders, A.W. Caswell, S. Roy, D.H. Plemmons, J.R. Gord, 50-kHz-rate 2D imaging of temperature and H₂O concentration at the exhaust plane of a J85 engine using hyperspectral tomography. *Opt. Express* **21**, 1152–1162 (2013)

20. J.C. McDaniel, C.P. Goyne, E.B. Bryner, D.B. Le, C.T. Smith, R.H. Krauss, in *Dual-Mode Scramjet Operation at a Mach 5 Flight Enthalpy in a Clean Air Test Facility. AIP Conference Proceedings*, vol. 762 (AIP, 2005), pp. 1277–1282
21. M. Gruber, J. Donbar, Mixing and combustion studies using cavity-based flameholders in a supersonic flow. *J. Propuls. Power* **20**, 769–778 (2004)
22. A. Ben-Yakar, R. Hanson, Cavity flame-holders for ignition and flame stabilization in scramjets: an overview. *J. Propuls. Power* **17**, 869–877 (2001)
23. C.S. Goldenstein, I.A. Schultz, R.M. Spearrin, J.B. Jeffries, R.K. Hanson, Scanned-wavelength-modulation spectroscopy near 2.5 μm for H_2O and temperature in a hydrocarbon-fueled scramjet combustor. *Appl. Phys. B* (2013). doi:[10.1007/s00340-013-5755-0](https://doi.org/10.1007/s00340-013-5755-0)
24. I.A. Schultz, C.S. Goldenstein, R.M. Spearrin, J.B. Jeffries, R.K. Hanson, Multispecies mid-infrared absorption measurements in a hydrocarbon-fueled scramjet combustor. *J. Propuls. Power* (2014) (accepted)